2017

Benchmark Burnishing with Almen Strip for Surface Integrity

Z. Y. Liu
University of Alabama - Tuscaloosa

C. H. Fu
University of Alabama - Tuscaloosa

M. P. Sealy
University of Nebraska-Lincoln, sealy@unl.edu

Y. Zhao
Shandong University of Technology

Y. B. Guo
University of Alabama - Tuscaloosa, yguo@eng.ua.edu

Available online at www.sciencedirect.com

ScienceDirect

Procedia Manufacturing 10 (2017) 456 – 466

Procedia MANUFACTURING

45th SME North American Manufacturing Research Conference, NAMRC 45, LA, USA

Benchmark Burnishing with Almen Strip for Surface Integrity

Z.Y. Liu[a], C.H. Fu[a], M.P. Sealy[b], Y. Zhao[c], and Y.B. Guo[a]*

[a] *Dept. of Mechanical Eng., The University of Alabama, Tuscaloosa, AL, 35487, U.S.A*
[b] *Dept. of Mechanical and Materials Eng., University of Nebraska, Lincoln, NE 68588, U.S.A.*
[c] *School of Mechanical Engineering, Shandong University of Technology, Zibo 255049, China*

Abstract

Burnishing is a surface treatment process widely used in aerospace, navy and other industries to improve fatigue and corrosion resistance by introducing a compressive residual stress layer. The measurement of residual stress by XRD is expensive, time consuming, and tedious. This work presented a quick method to determine the residual stress by using Almen strips. Inspired by the application of Almen strips in shot peening, deflections of burnished Almen strips under different burnishing conditions were measured. It was found that the deflection of Almen strip reflects the magnitude and penetration depth into subsurface of induced stress. Higher burnishing force, smaller feed, and smaller ball diameter tend to produce more deflection, which indicates more compressive residual stress.

Peer-review under responsibility of the organizing committee of the 45th SME North American Manufacturing Research Conference

Keywords: Burnishing; Almen strip; Residual stress; Surface integrity

1. Introduction

Burnishing is a surface treatment process widely used in aerospace, navy and other industries. The process introduces a compressive residual stress layer on the burnished surface [1]. The depth of the compressive layer can exceed 1 mm, which is much deeper than shot peening. Thus burnishing can significantly improve high cycle fatigue and corrosion resistance [2, 3]. Burnishing has been successfully applied to many engineering materials

* Corresponding author. Tel.: +1-205-348-2615; fax: +1-205-348-6419.
E-mail address: yguo@eng.ua.edu

Peer-review under responsibility of the organizing committee of the 45th SME North American Manufacturing Research Conference
doi:10.1016/j.promfg.2017.07.027

including steels [4], Inconel [5], titanium alloys [6], and biomedical materials such as nitinol [7], and magnesium alloy [8].

The residual stress distribution plays a significant role on the functionality of a burnished part. The measurement of residual stress is critical for quality assurance. However, the traditional methods such as X-Ray diffraction (XRD) are expensive, time consuming, and tedious [9]. In order, a lot of experimental work needs to be done. A cost-effective and efficient method is needed to find the relationship between process space and residual stress distribution.

Almen strip provides a potential quick method to determine residual stress. Almen intensity is widely used in shot peening to ensure the effectiveness and repeatability. The method was introduced by Almen and Black [10]. The intensity is quantified by measuring the deflection of peened SAE 1070 strips (Almen strip). Due to the residual stress induced by shot peening, Almen strips bend toward the peening direction after release from holder. The arc height (i.e., deflection) can be easily measured and defined as Almen intensity. The dimensions of Almen strips are standardized with length of 76.20 mm, width of 19.05 mm and three available thickness (type A: 1.29 mm, type N: 0.79 mm, and type C: 2.39 mm). The Almen intensity has the advantage that it combines the effects of all the process parameters (peening pressure, shot size, shot material, nozzle size) into one measurement, providing a quick and cost effective testing method for repeatability of the process.

Similar to shot peening, residual stress induced by burnishing is controlled by a set of process parameters including burnishing pressure, burnishing ball size, feed and burnishing pattern. Inspired by the successful application of Almen strip in shot peening, this study aims to investigate residual stress by burnishing Almen strips and measuring the strip deflections. It may provide a fast method to the test of repeatability of residual stress in burnishing process.

The objectives of this research are to: (a) investigate the effect of burnishing conditions on the deflection of Almen strip; and (b) assess the feasibility of using Almen strip in burnishing process.

2. Burnishing Experiment

The burnishing experimental (Fig. 1) was conducted using a Cincinnati arrow 500 CNC machine. The Ecoroll tool with a ceramic ball was used. The ceramic ball rolled over the workpiece surface under the applied hydraulic pressure. A load cell was used to measure the burnishing force.

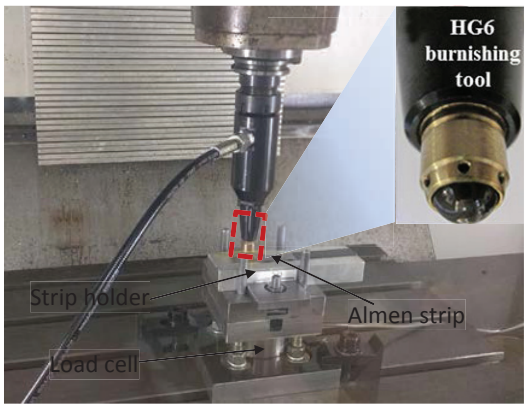

Fig. 1. Experiment setup.

The experiment design was summarized in Table 1. A constant linear speed of 3000 mm/min was used in the experiment. The effect of burnishing force, feed, ball diameter, and pattern was investigated. The schematic of vertical and horizontal patterns on strip deflection and residual stress is shown in Fig. 2. The burnishing direction for

vertical pattern is perpendicular to the length direction of the strip, and vice versa. Each burnishing condition was repeated three times to ensure experiment repeatability.

After burnishing, the Almen strip was removed from the strip holder. The arc height of deflected strip was measured with an Almen strip gauge (Fig. 3). Surface roughness of burnished strip was also measured. Each burnishing strip was measured three times. At each burnishing condition, one sample is sectioned, mounted, and polished. The microhardness at subsurface was measured using a Vickers indenter.

Table 1. Burnishing experimental design

Case #	Burnishing force *F* (N)	Feed *f* (mm)	Ball diameter *D* (mm)	Speed *v* (mm/min)	Pattern
1	49	0.10	6	3000	Vertical
2	98	0.10	6	3000	Vertical
3	196	0.10	6	3000	Vertical
4	294	0.10	6	3000	Vertical
5	390	0.10	6	3000	Vertical
6	196	0.05	6	3000	Vertical
7	196	0.15	6	3000	Vertical
8	196	0.20	6	3000	Vertical
9	196	0.25	6	3000	Vertical
10	196	0.10	6	3000	Horizontal
11	98	0.10	3	3000	Vertical
12	98	0.10	12.7	3000	Vertical

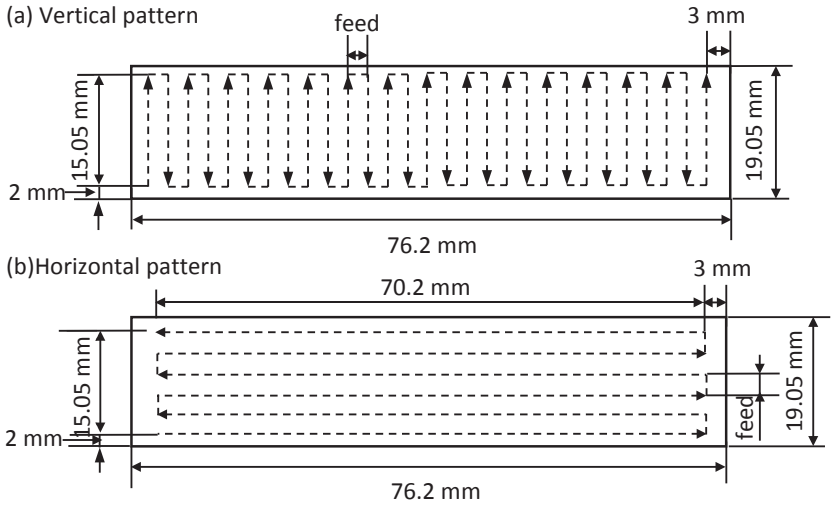

Fig. 2. Burnishing patterns: (a) vertical, (b) horizontal.

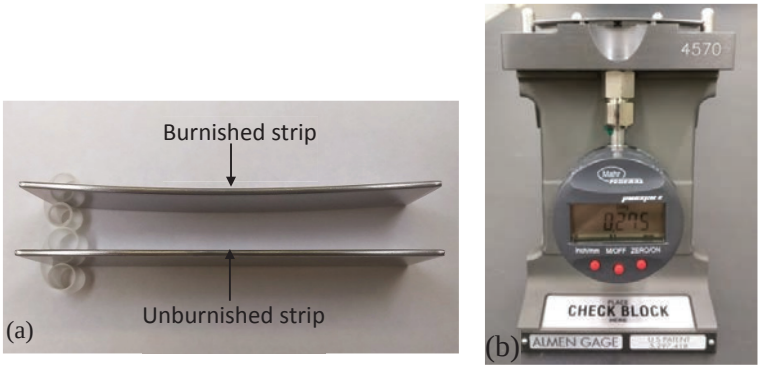

Fig. 3. Strip deflection measurement: (a) burnished vs. unburnished strips, (b) arc height measurement with Almen strip gauge.

3. Calculation Method of Residual Stress and Almen Strip Deflection

The schematic of calculating residual stress and strip deflection are shown in Fig. 4. Three different stress states were investigated in this study.

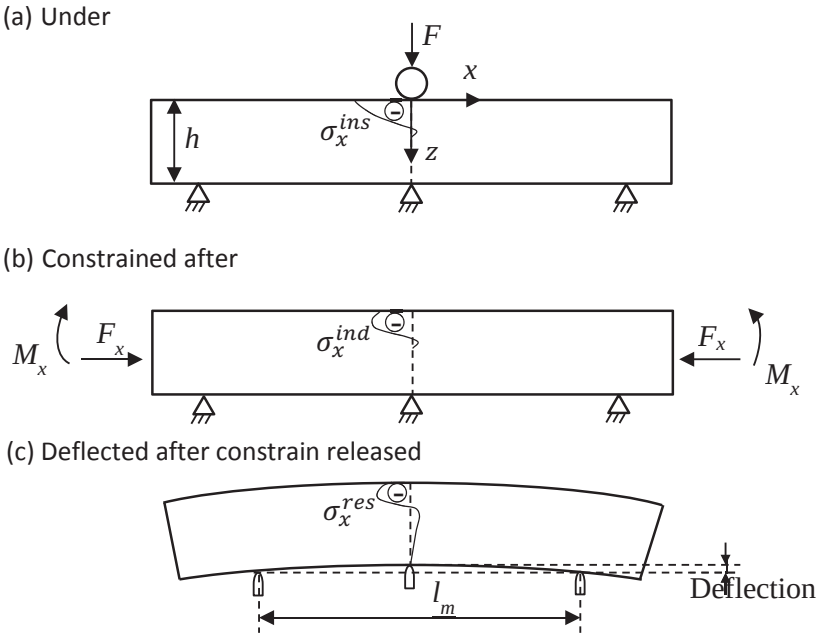

Fig. 4. Schematic of calculating residual stress and strip deflection: (a) instantaneous stress during burnishing, (b) induced stress after burnishing in constrained strip, (c) residual stress after releasing constraints.

- Instantaneous stress σ_{ins}: the stress in the strip during burnishing, i.e., the contact stress applied by burnishing ball.
- Induced stress σ_{ind}: the stress in the strip after burnishing in constrained strip.
- Residual stress σ_{res}: the stress in the strip after releasing constraints.

3.1. Instantaneous stress

Hertz theory of elastic contact theory was used to characterize the applied burnishing load as a reference model (Eqs. 1-5) [11]. The contact radius, pressure and penetration depth can be calculated given the material properties and geometry of burnishing ball and Almen strip.

$$E^* = \left(\frac{1-\nu_1^2}{E_1} + \frac{1-\nu_2^2}{E_2}\right)^{-1} \tag{1}$$

$$\frac{1}{R} = \left(\frac{1}{R_1} + \frac{1}{R_2}\right) \tag{2}$$

$$a = \left(\frac{3PR}{4E^*}\right)^{1/3} \tag{3}$$

$$p_0 = \frac{3P}{2\pi a^2} \tag{4}$$

$$\delta = \left(\frac{9P^2}{16RE^{*2}}\right)^{1/3} \tag{5}$$

where E^*, effective modulus; E_1, Young's modulus of the burnishing ball; E_2, Young's modulus of Almen strip; ν_1, Poisson's ratio of burnishing ball; ν_2, Poisson's ratio of Almen strip; R, effective curvature; R_1, curvature of burnishing ball; R_2, curvature of workpiece, which equals infinity for flat surface; P, applied load; P_0, maximum contact pressure, a, contact radius.

The stresses $\sigma_x(z)$, $\sigma_y(z)$, $\sigma_z(z)$ and τ along the z-axis passing through the center of the burnishing ball are calculated by Eqs. 6-10 [11]. Since the stresses are calculated based on elastic theory, the actual stress will be different from the calculation. However, the calculation provides valuable insight into the burnishing process. For example, the depth of plastic deformation can be analyzed by investigating the shear stress.

$$\sigma_x(z) = \sigma_y(z) = -p_0\left[-\frac{1}{2}A(z) + (1+\nu_2)B(z)\right] \tag{6}$$

$$\sigma_z = -p_0 A(z) \tag{7}$$

$$\tau = p_0 a[z - z^2(a^2 - z^2)^{-1/2}] \tag{8}$$

$$A(z) = \left[1 + \left(\frac{z}{a_e}\right)^2\right]^{-1} \tag{9}$$

$$B(z) = 1 - \frac{z}{a_e}\tan^{-1}\left(\frac{a_e}{z}\right) \tag{10}$$

3.2. Induced stress

Due to the high contact load induced by the burnishing ball, plastic deformation is induced since Hertz contact stress far exceeds the material yield strength. The stress state in the strip (denoted as induced stress σ_x^{ind}) is not in an equilibrium condition. The relationship between the stress distribution and constraint force applied by the Almen strip holder after burnishing under constraints is given in Eq. 11 and Eq. 12.

$$\int_0^h \sigma_x^{ind} b dz + F_x = 0 \tag{11}$$

in which, b and h are the width and thickness of an Almen strip, respectively.

$$\int_0^h \sigma_x^{ind} \left(\frac{h}{2} - z\right) b dz + M_x = 0 \tag{12}$$

3.3. Residual stress

When the constraints are released, the stress will be redistributed and the strip will be deflected because of the residual stress. The deflection d (i.e., arc height) of the strip (the Almen intensity measured by Almen intensity gauge) can be given by Eq. 13. The residual stress is given by Eq. 14.

$$d = \frac{3M_x l_m^2}{2E_2 b h^3} \tag{13}$$

$$\sigma_x^{res} = \sigma_x^{ind} + \frac{F_x}{A} + \frac{M_x \left(\frac{h}{2} - z\right)}{I} \tag{14}$$

where l_m is the reference distance for measuring Almen intensity. E_2, A, and I are the elastic modulus, cross-section area, and moment of inertia of the Almen Strip, respectively. It should be noted that for the vertical pattern, the arc height is determined by residual stress perpendicular to burnishing direction, and vice versa.

From Eq. 12 and Eq. 13, it can be seen that the deflection influenced by both the magnitude and the penetration depth of the induced stress. In other words, the arc height reflects the induced stress magnitude and penetration depth.

4. Results and Discussion

4.1. Deflection of Almen strip

The effect of burnishing force on deflection of the Almen strip is shown in Fig. 5. Arc height increases with increasing burnishing force. A larger force produces more plastic deformation which generates larger compressive residual stress. As a result, a larger force produces larger deflection.

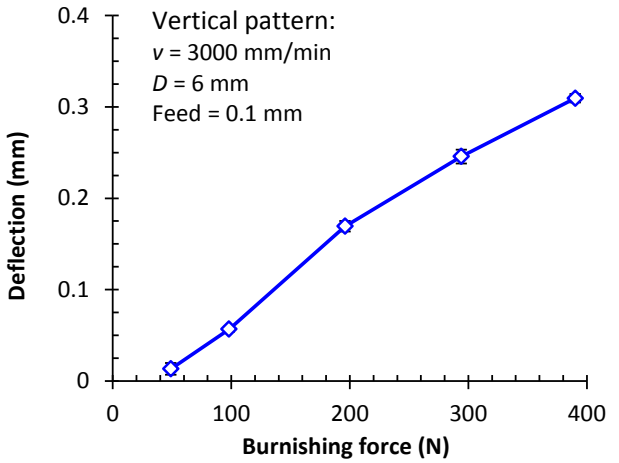

Fig. 5. The effect of burnishing force on strip deflection.

Fig. 6 shows the effect of feed on deflection of Almen strip. For an identical burnishing area, the number of burnishing pass is inversely proportional to the feed. More passes are required to for the burnished area with smaller feed, which leads to more surface plastic deformation, and, therefore, more compressive residual stress and larger deflection.

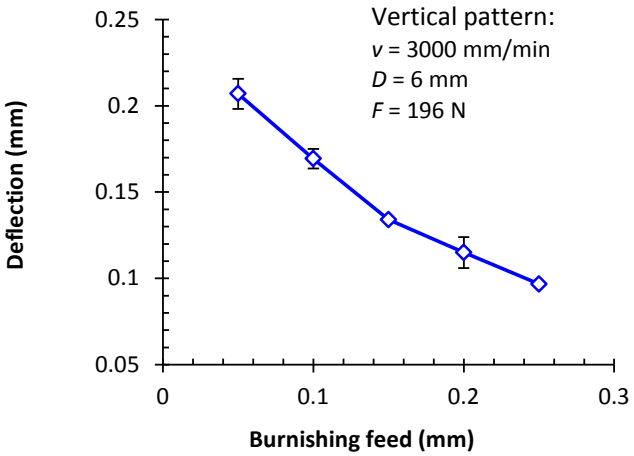

Fig. 6. The effect of feed on strip deflection.

Fig. 7. shows the effect of burnishing pattern on deflection of the Almen strip. For the burnishing conditions used in this experiment, the vertical pattern produces larger deflection than the horizontal pattern. As mentioned in in section 3, the deflection for vertical pattern is determined by residual stress at feed direction, and verse vice. Thus residual stress at feed direction would be more compressive than burnishing direction. Thus burnishing of Almen strip provides a fast method to determine the anisotropy of residual stress. Based on the deflection from the two burnishing patterns, one can select the favorable burnishing pattern based on loading condition for different service environments.

The effect of ball size on the strip deflection is shown in Fig. 8. The deflection decreases with increasing ball diameter. From the perspective of contact mechanics, a small ball tends to generate higher contact stress and

produce larger plastic deformation, which may result in more compressive residual stress and therefore, larger deflection.

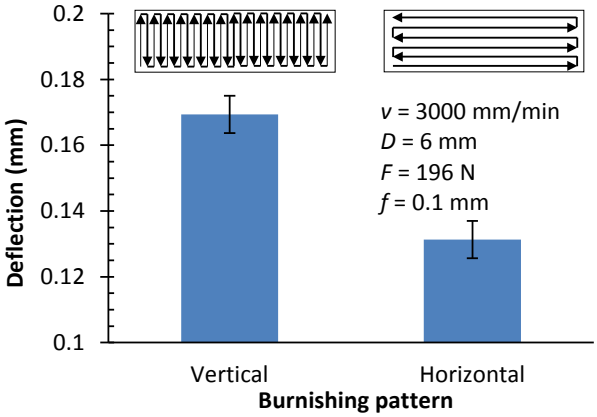

Fig. 7. The effect of burnishing pattern on strip deflection.

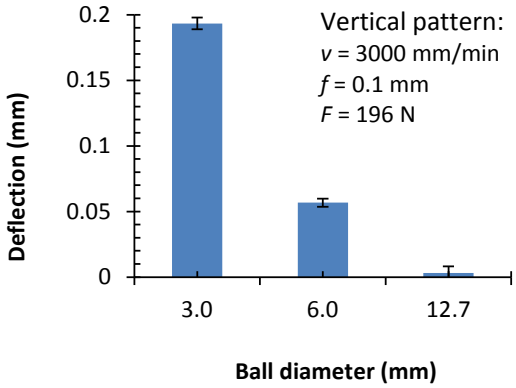

Fig. 8. The effect of ball diameter on deflection.

4.2. Surface roughness

The effect of burnishing load on surface roughness is shown in Fig. 9. The surface roughness at feed direction was smaller than burnishing direction. At feed direction, the roughness is the highest when burnishing force was 196 N. The surface roughness by lower burnishing force or higher burnishing force is small. At burnishing direction, surface roughness decreases with higher burnishing force.

Fig. 10 shows the effect of burnishing feed on surface roughness. The surface roughness at feed direction was smaller than burnishing direction except the case feed = 0.15 mm. At burnishing direction, the roughness increases with the feed. At feed direction, the surface roughness is the highest when feed is 0.15 mm.

The effect of ball diameter on surface roughness is shown in Fig. 11. At feed direction, the surface roughness for different ball sizes is almost the same. At burnishing direction, the surface roughness increases with the ball size. Once again, surface roughness at feed direction is smaller than burnishing direction. By comparing the surface roughness and deflection produced by different burnishing conditions, it can be found that the relationship between surface roughness and residual stress is very weak.

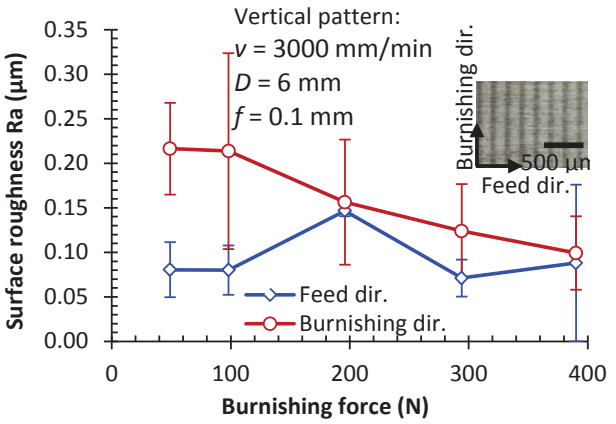

Fig. 9. Effect of burnishing force on surface roughness.

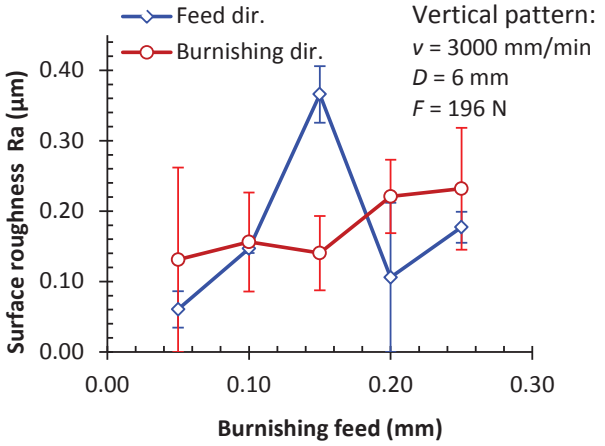

Fig. 10. Effect of feed on surface roughness profile.

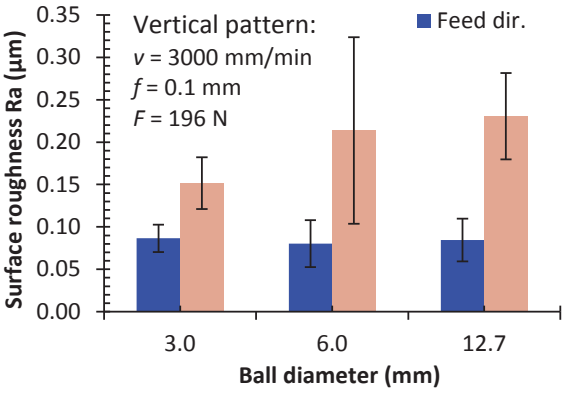

Fig. 11. Effect of ball diameter on surface roughness.

4.3. Microhardness

The effect of burnishing force, feed, and ball diameter on microhardness is shown in Figs. 12-14, respectively. The microhardness increases with the decrease of burnishing force and feed. Burnishing ball with diameter of 6 mm produces lowest hardness. The microhardness produced by ball diameter of 3 and 12.7 mm is similar. The general observation from the three figures shows that microhardness increases with the increased depth in the subsurface, which implies that burnishing produces maximum compressive stress in subsurface. The microhardness reaches a stabilized value at a depth of 100 μm.

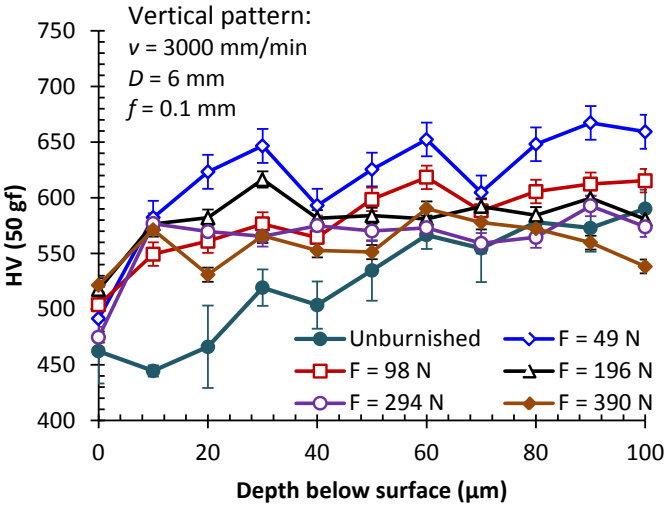

Fig. 12. Effect of burnishing force on microhardness profile.

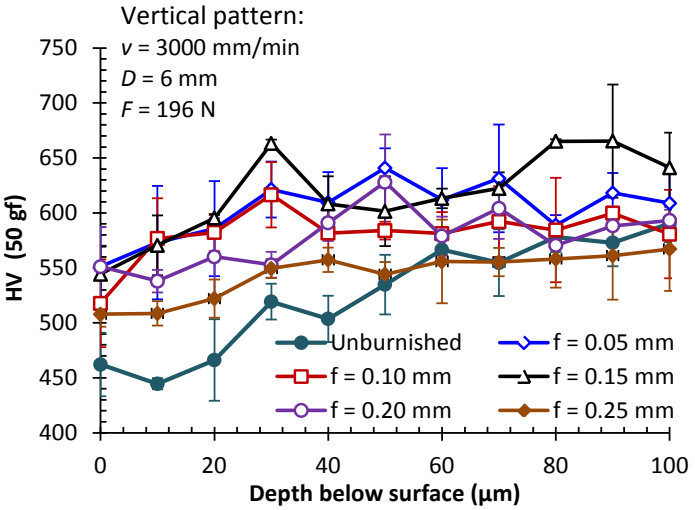

Fig. 13. Effect of feed on microhardness profile.

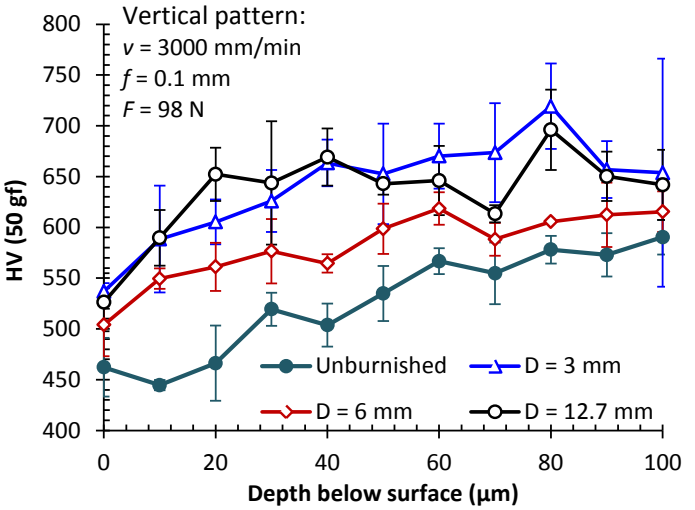

Fig. 14. Effect of ball diameter on microhardness profile.

5. Conclusions

This research initiated the feasibility of using Almen strip in burnishing process. The effect of burnishing conditions on deflection, surface roughness, and microhardness of the Almen strip was investigated. Hertz contact theory was used to characterize the loading conditions. The key conclusions are summarized as follows:

- The deflection of Almen strip reflects the magnitude and penetration depth into subsurface of induced stress, which provides a fast method to test the effectiveness of burnishing process.
- Higher burnishing force, smaller feed, and smaller ball diameter tend to produce more deflection, which indicates more compressive residual stress.
- The deflection of Almen strip under the vertical and horizontal burnishing patterns provides a fast method to determine the relative magnitude of residual stress at feed and burnishing directions.

References

[1] Klocke, F. and Liermann, J., 1998. Roller Burnishing of Hard Turned Surfaces. *International Journal of Machine Tools and Manufacture*, 38(5), pp. 419-423.
[2] Prevéy, P. S., Jayaraman, N. & Cammett, J., 2005. Overview of Low Plasticity Burnishing for Mitigation of Fatigue Damage Mechanisms. In *Proceedings of ICSP 9*, pp. 1-6.
[3] Salahshoor, M. and Guo, Y. B., 2012. Biodegradable Orthopedic Magnesium-Calcium (MgCa) Alloys, Processing, and Corrosion Performance. *Materials*, 5(1), pp. 135-155.
[4] El-Axir, M. H., 2000. An Investigation into Roller Burnishing. *International Journal of Machine Tools and Manufacture*, 40(11), pp. 1603-1617.
[5] Prevéy, P., Telesman, J., Gabb, T. & Kantzos, P., 2000. FOD Resistance and Fatigue Crack Arrest in Low Plasticity Burnished IN718. In *Proceedings of the 5th National Turbine Engineering HCF Conference*.
[6] Prevéy, P. S., Shepard, M. J. & Smith, P. R., 2001. The Effect of Low Plasticity Burnishing (LPB) on the HCF Performance and FOD Resistance of Ti-6Al-4V. In *6th National Turbine Engine High Cycle Fatigue (HCF) Conference*, pp. 1-10.
[7] Fu, C. H., Sealy, M. P., Guo, Y. B. and Wei, X. T., 2014. Austenite–Martensite Phase Transformation of Biomedical Nitinol by Ball Burnishing. *Journal of Materials Processing Technology*, 214(12), pp. 3122-3130.
[8] Salahshoor, M. and Guo, Y. B., 2011. Surface Integrity of Biodegradable Magnesium–Calcium Orthopedic Implant by Burnishing. *Journal of the Mechanical Behavior of Biomedical Materials*, 4(8), pp. 1888-1904.
[9] Rossini, N. S., Dassisti, M., Benyounis, K. Y. and Olabi, A. G., 2012. Methods of Measuring Residual Stresses in Components. *Materials & Design*, 35, pp. 572-588.
[10] Almen, J.O. & Black, P.H., 1963. *Residual Stresses and Fatigue in Metals*, McGraw-Hill.
[11] Johnson, K., 1987. *Contact Mechanics*, Cambridge University Press.